

# RSC Advances



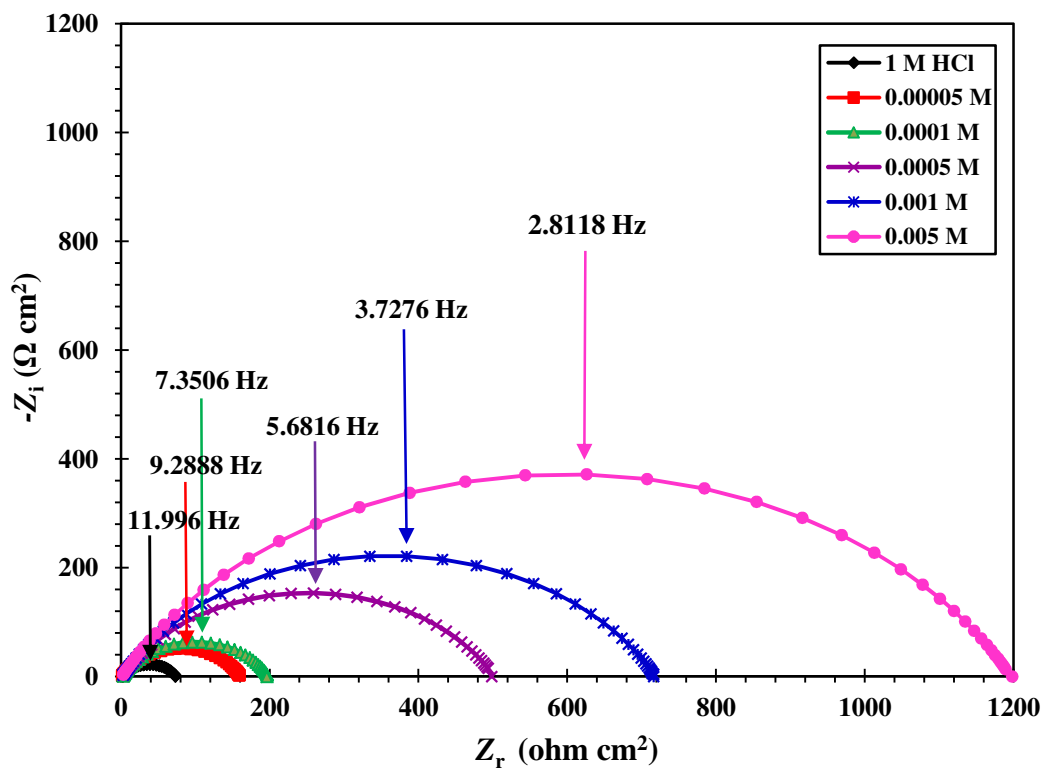
This is an *Accepted Manuscript*, which has been through the Royal Society of Chemistry peer review process and has been accepted for publication.

*Accepted Manuscripts* are published online shortly after acceptance, before technical editing, formatting and proof reading. Using this free service, authors can make their results available to the community, in citable form, before we publish the edited article. This *Accepted Manuscript* will be replaced by the edited, formatted and paginated article as soon as this is available.

You can find more information about *Accepted Manuscripts* in the [Information for Authors](#).

Please note that technical editing may introduce minor changes to the text and/or graphics, which may alter content. The journal's standard [Terms & Conditions](#) and the [Ethical guidelines](#) still apply. In no event shall the Royal Society of Chemistry be held responsible for any errors or omissions in this *Accepted Manuscript* or any consequences arising from the use of any information it contains.

## Graphical abstract



## Research Highlights

1. Novel cationic surfactant has good surface properties.
2. Novel cationic surfactant is a good inhibitor for carbon steel in 1 M HCl solution.
3. By increase of the inhibitor concentration the inhibition efficiency increases.
4. The techniques include weight loss, potentiodynamic polarization and EIS.
5. Inhibitor act as a mixed-type inhibitor and its adsorption obeys Langmuir isotherm.

# Studying the corrosion inhibition of carbon steel in hydrochloric acid solution by 1-dodecyl-methyl-1*H*-benzo[*d*][1,2,3]triazole-1-ium bromide

M.A. Hegazy<sup>a,\*</sup>, S.S. Abd El Rehim<sup>b</sup>, A.M. Badawi<sup>a</sup>, M.Y. Ahmed<sup>c</sup>

<sup>a</sup>*Egyptian Petroleum Research Institute (EPRI), Nasr City, Cairo, Egypt*

<sup>b</sup>*Ain Shams University, Faculty of Science, Cairo, Egypt*

<sup>c</sup>*Science and Technology Center of Excellence ( STCE ), Cairo, Egypt*

## Abstract

A novel cationic surfactant 1-dodecyl-methyl-1*H*-benzo[*d*][1,2,3]triazole-1-ium bromide (1-DMBT) was synthesized and its structure was confirmed by using <sup>1</sup>HNMR and FTIR spectroscopic analysis. The surface tension and electrical conductivity of that surfactant were measured and its critical micelle concentration and some of its surface properties also were determined and discussed. The inhibition performance of the prepared (1-DMBT) on the corrosion of carbon steel in 1.0 M HCl solution was investigated at different concentrations and temperatures by using weight loss, potentiodynamic polarization and electrochemical impedance spectroscopy. The obtained results revealed that the synthesized (1-DMBT) regards as a good corrosion inhibitor for carbon steel in HCl medium and acts mainly as a mixed-type inhibitor. The inhibition of (1-DMBT) efficiency increases with increasing its concentration but decreases with rise in temperature. Such inhibition is related to the adsorption of the surfactant on the metal surface and the adsorption process obeys the Langmuir isotherm.

**Keywords:** Cationic surfactants; Acid inhibition; Adsorption; Thermodynamic.

---

\* Corresponding author. Tel.: +20 1002653529; fax: +20 222747433.

E-mail address: [mohamed\\_hgazy@yahoo.com](mailto:mohamed_hgazy@yahoo.com) (M.A. Hegazy).

## 1. Introduction

Acidic solutions are generally used for the removal of rust and scales in pickling and petroleum industry [1-6]. Inhibitors are generally added to acid solutions used in these processes to control the metal dissolution. In addition, the most practical methods for protection against corrosion are the use of inhibitors especially in acidic media [7-8]. Most well-known acid corrosion inhibitors are organic compounds containing nitrogen, sulfur, and oxygen atoms; nitrogen-containing organic compounds are known to be efficient corrosion inhibitors in HCl solutions, while sulfur-containing compounds are sometimes preferred for H<sub>2</sub>SO<sub>4</sub> solutions [8,9]. Among the various nitrogenous compounds used as inhibitors, triazoles are considered as environmental acceptable chemicals [10-14]. Many substituted triazole derivatives have been recently studied in considerable details as effective corrosion inhibitors for steel in acidic media [15–18]. The first step in the action of these compounds in acidic media is their adsorption on the metal surface [19-23].

In the present work, we synthesized a new cationic surfactant based on tolyl triazole namely 1-dodecyl-methyl-1*H*-benzo[*d*][1,2,3]triazole-1-ium bromide (1-DMBT), this surfactant was tested as a novel inhibitor for corrosion of carbon steel in 1.0 M HCl media at different inhibitor concentrations and temperatures using weight loss method. The inhibitive activity of 1-DMBT also was examined via potentiodynamic polarization and (EIS) methods. Critical micelle concentration ( $C_{cmc}$ ) and some surface properties of this novel inhibitor at 25 °C was determined and discussed.

## 2. Materials and experimental techniques

### 2.1. Materials

The tested inhibitor, namely 1-dodecyl-methyl-1*H*-benzo[*d*][1,2,3]triazole-1-ium bromide, was synthesized from reaction of one mol 5-methyl-1*H*-benzo[*d*][1,2,3]triazole with one mol

1-bromododecane in ethanol at 70 °C for 24 h. The mixture was allowed to cool-down. The obtained pale brown precipitate product was further purified by diethyl ether then recrystallized from ethanol to form a white precipitate is of 1-dodecyl-5-methyl-1H-benzo[d][1,2,3]triazol-1-ium bromide. The chemical composition of the used carbon steel in the present work is given in Table 1. All solutions used were freshly prepared from analar chemicals and doubly-distilled water. Chemical structure of the synthesized inhibitor (Fig. 1) was confirmed by FTIR and <sup>1</sup>H NMR spectroscopy. FTIR analysis was carried out using ATI Mattson infinity series TM, Bench top 961 controlled by Win First TM V2.01 software. <sup>1</sup>H NMR analysis was measured in DMSO-d<sub>6</sub> using Joel ECA 500 MHZ NMR spectrometer.

## 2.2. Surface tension and conductivity measurements

Surface tension ( $\gamma$ ) was measured by Du Nouy Tensiometer (Kruss Type 6) for various concentrations of synthesized surfactant 1-DMPT solutions. Doubly distilled water with a surface tension of 72 mN m<sup>-1</sup> at 25 °C was used to prepare all surfactant solutions used. Surface tension ( $\gamma$ ) of 1-DMPT at any concentration used was determined.

An electrical conductivity meter (Type 522; Crison Instrument, S.A.) was used to measure the conductivity of surfactant solutions. Measurements were performed in a jacketed cell of knowing cell constant at 25±1°C.

## 2.3. Corrosion measurements

### Weight loss measurements

Firstly, the carbon steel sheets of 3 cm × 6 cm × 0.5 cm were polished successively with a series of emery papers (grades 320–500–800–1000–1200) washed with distilled water, degreased with acetone and finally dried at room temperature. The weight loss (mg cm<sup>-2</sup>) was determined by weighing the clean sheets before and after immersion in naturally aerated stagnant 1.0 M HCl solution without and with a given concentration of the inhibitor run for

24 h at a given temperature  $\pm 1$  °C with help of an air thermostat. Each one was carried out in triplicate and the average value of the weight loss is reported.

### Electrochemical measurements

Electrochemical experiments were conducted by using an Autolab 302 N. A conventional three-electrode cell containing a reference electrode (Ag/AgCl), a platinum wire counter electrode, and the working electrode. The working electrode was made from carbon steel rod with the same composition as given in Table 1. The rod is embedded in PVC holder using epoxy resin so that only its cross-section area ( $0.358 \text{ cm}^2$ ) was exposed to the test solution. In each run, a clean set of electrodes and a freshly prepared solution was used at  $25 \pm 1$  °C. Potentiodynamic polarization was performed by changing the electrode potential automatically (from -800 to -200 mV vs. Ag/AgCl) with a scan rate of  $0.2 \text{ mV s}^{-1}$ . The impedance experiments were carried out at a frequency range (100k Hz to 0.2 Hz) with an amplitude of 4 mV peak-to-peak using ac signals at open circuit potentials and  $25 \pm 1$  °C.

## 3. Results and discussion

### 3.1. Characterization of the synthesized 1-DMPT

The chemical structure of the synthesized cationic surfactant in the Fig. 1 was confirmed by  $^1\text{H}$  NMR,  $^{13}\text{C}$  NMR, and FTIR spectra.

#### $^1\text{H}$ NMR spectrum

The  $^1\text{H}$  NMR spectrum of the prepared surfactant is shown in Fig. 2. The spectrum revealed different bands at  $\delta = 0.861$  ppm (t, 3H,  $\text{CH}_3(\text{CH}_2)_9\text{CH}_2\text{CH}_2\text{N}$ );  $\delta = 1.216$  (m, 18H,  $\text{CH}_3(\text{CH}_2)_9\text{CH}_2\text{CH}_2\text{N}$ );  $\delta = 1.635$  (m, 2H,  $\text{CH}_3(\text{CH}_2)_9\text{CH}_2\text{CH}_2\text{N}$ );  $\delta = 2.009$  (m, 2H,  $\text{CH}_3(\text{CH}_2)_9\text{CH}_2\text{CH}_2\text{N}$ );  $\delta = 3.353$  (s, 3H,  $\text{CH}_3\text{Ar}$ );  $\delta = 7.864$  (d, 1H, 4-ArH);  $\delta = 8.264$  (d, 2H, 3,6-ArH);  $\delta = 8.340$  (s, 1H, NH) the data of  $^1\text{H}$  NMR spectrum confirmed the expected hydrogen proton distribution in the synthesized 1-DMPT.

### <sup>13</sup>C NMR spectrum

<sup>13</sup>C NMR (DMSO) spectrum of 1-DMBT is shown in Fig. 3. The spectrum showed different bands at  $\delta=13.756$  ppm (NCH<sub>2</sub>CH<sub>2</sub>CH<sub>2</sub>(CH<sub>2</sub>)<sub>7</sub>CH<sub>2</sub>CH<sub>3</sub>);  $\delta=16.792$  ppm (NCH<sub>2</sub>CH<sub>2</sub>CH<sub>2</sub>-(CH<sub>2</sub>)<sub>7</sub>CH<sub>2</sub>CH<sub>3</sub>);  $\delta=39.250$  ppm (NCH<sub>2</sub>CH<sub>2</sub>CH<sub>2</sub>(CH<sub>2</sub>)<sub>7</sub>CH<sub>2</sub>CH<sub>3</sub>);  $\delta=28.671$  ppm (NCH<sub>2</sub>CH<sub>2</sub>CH<sub>2</sub>(CH<sub>2</sub>)<sub>7</sub>CH<sub>2</sub>CH<sub>3</sub>);  $\delta=21.303$  ppm (NCH<sub>2</sub>CH<sub>2</sub>CH<sub>2</sub>(CH<sub>2</sub>)<sub>7</sub>CH<sub>2</sub>CH<sub>3</sub>);  $\delta=58.142$  ppm (NCH<sub>2</sub>CH<sub>2</sub>CH<sub>2</sub>(CH<sub>2</sub>)<sub>7</sub>CH<sub>2</sub>CH<sub>3</sub>); 111.814, 115.050, 125.169, 127.195, 135.637, 138.164 ppm (6 sets of toluidine-C); 25.496 ppm (Ar-CH<sub>3</sub>). The data of <sup>13</sup>C NMR spectrum confirmed the expected carbon distribution in the synthesized 1-DMBT.

### FTIR spectrum

The FTIR spectrum of 1-DMBT is presented in Fig. 4. The data showed the following absorption bands at 716.86 cm<sup>-1</sup> (CH<sub>2</sub> rocking), 1361.40 cm<sup>-1</sup> (CH<sub>2</sub> deformation), 2851.50 cm<sup>-1</sup> (CH stretching), 1035.63 (C-N<sup>+</sup>), other band at 1117.22 cm<sup>-1</sup> corresponding to (C-N), 818.76 P-substitution of benzene ring, 1610.04 cm<sup>-1</sup> (CH stretching) of benzene, 1461.31 cm<sup>-1</sup> (CH bending) of benzene. The FTIR spectrum confirmed the expected function groups in the prepared surfactant 1-DMBT.

## 3.2. Surface active properties

### The surface tension

The surface tension ( $\gamma$ ) of solutions containing different concentrations of 1-DMBT( $C$ ) below and above its critical micelle concentration ( $C_{cmc}$ ) was measured at 25 °C. A representative plot of  $\gamma$  vs  $-\log C$  of is shown in Fig. 4. It is clear that the surface tension decreases linearly with increasing the concentration of the surfactant up to its  $C_{cmc}$ . But after  $C_{cmc}$ , the surface tension tends to remain nearly constant. This is a common behavior shown by surfactants in their solutions and is used to determine their micelle concentrations. The value of ( $C_{cmc}$ ) of 1-DMBT obtained by this method is given in Table 2.



Some surface properties such as maximal surface pressure ( $\pi_{\text{cmc}}$ ), surface excess ( $\Gamma_{\text{max}}$ ) and area per molecule ( $A_{\text{min}}$ ) of 1-DMBT were calculated using the data obtained from the surface tension measurements. The value of  $\pi_{\text{max}}$  was calculated using the following equation: [24].

$$\pi_{\text{cmc}} = \gamma_0 - \gamma_{\text{cmc}} \quad (1)$$

where  $\gamma_0$  and  $\gamma_{\text{cmc}}$  are the surface tensions of pure water and that of the surfactant solution containing its  $C_{\text{cmc}}$  at 25 °C, respectively. The calculated value of  $\pi_{\text{cmc}}$  is listed in Table 2.

The slope of the straight line in the surface tension plot ( $dy / d\log C$ ) below  $C_{\text{cmc}}$ , was used to calculate the surface excess concentration of surfactant ions,  $\Gamma_{\text{max}}$ , using the Gibbs adsorption equation [25]:

$$\Gamma_{\text{max}} = -\left(\frac{1}{nRT}\right)\left(\frac{dy}{d\log C}\right) \quad (2)$$

where  $\Gamma_{\text{max}}$  is the surface excess concentration of surfactant ions,  $R$  is gas constant,  $T$  is absolute temperature,  $C$  is concentration of surfactant,  $\gamma$  is surface tension at given concentration, and  $n$  is number of species ions in solution.

The value of surface excess concentration was calculated and is listed in Table 2. It was found that the value of surface excess concentration value is high which could be due to the hydrophobic effect of the large carbon chain [26].

The minimal surface area per adsorbed molecule, ( $A_{\text{min}}$ ) can be obtained as follows:

$$A_{\text{min}} = \frac{10^{14}}{\Gamma_{\text{max}}N_A} \quad (3)$$

where  $N_A$  is the Avogadro's number and  $\Gamma_{\text{max}}$  is the maximal surface excess of the adsorbed surfactant actions at the interface [27].

The value of the area per molecule was calculated and recorded in Table 2.

## Conductivity

The electrical conductivity ( $K$ ) of different concentrations of 1-DMPT solutions were performed at 25 °C. Plotting  $K$  vs concentration of concentration the surfactant gave two straight lines. One line for the concentration region below  $C_{cmc}$  and the second one above  $C_{cmc}$  concentration region [1, 13]. The intersection point between the straight lines gave the  $C_{cmc}$  while the ratio between the slopes of the two straight lines of the two concentration regions gave counter ion dissociation,  $\beta$ . Fig. 5 displays the  $K$ - $C$  of the prepared surfactant at 25 °C, from which value of  $\beta$  was calculated and is listed in Table 2. It was found that, there is an agreement between the values of  $C_{cmc}$  of 1-DMPT obtained using both surface tension and conductivity measurements.

## The standard free energy of micelle formation ( $\Delta G_m^0$ )

The  $C_{cmc}$  of a surfactant is regarded as a measure of the stability of its micellar form relative to its monomeric form. In the charged pseudophase model of micelle formation, the standard free energy of micelle formation per mole of surfactant ( $\Delta G_m^0$ ) is given by the following equation [28]:

$$\Delta G_m^0 = (2 - \beta) RT \ln(C_{cmc}) \quad (4)$$

where  $C_{cmc}$  is expressed in the molarity of the prepared surfactant and  $\beta$  is the counter ion dissociation obtained from conductivity measurements. From the above equation, the value of ( $\Delta G_m^0$ ) calculated and listed in Table 2. The negative sign of ( $\Delta G_m^0$ ) indicating that micelle formation is thermodynamically forward for the prepared surfactant with longer carbon chain, and the micellization process proceeds spontaneously.

## 3.3. Corrosion inhibition evaluation

### Potentiodynamic polarization

Fig. 6 illustrates the potentiodynamic anodic and cathodic polarization for carbon steel in naturally aerated and stagnant 1.0 M HCl in the absence and presence of various

concentrations of 1-DMBT at a scan rate  $0.2 \text{ mVs}^{-1}$  and  $25 \text{ }^\circ\text{C}$ . The addition of 1-DMBT to the acid solution reduces both the anodic and cathodic current densities indicating that the synthesized surfactant inhibits both the anodic dissolution of carbon steel and cathodic hydrogen evolution. The reduction in current densities enhances with increasing the concentration of the inhibitor. The Electrochemical kinetic parameters such corrosion potential ( $E_{\text{corr}}$ ), corrosion current density ( $j_{\text{corr}}$ ), cathodic and anodic line slopes ( $\beta_c$  and  $\beta_a$  respectively) were obtained from Tafel lines and are listed in Table 3. The results indicate that  $j_{\text{corr}}$  decreases with increasing the 1-DMPT concentration, suggesting that this surfactant functions as a corrosion inhibitor for carbon steel in HCl solution. The inhibition function of 1-DMPT is due to its adsorption on the electrode surface. The adsorbed species cover a fraction of the electrode surface and isolate it from the corrosion medium. The values of  $\beta_c$  and  $\beta_a$  are not significantly affected by changing the concentration of the inhibitor. This means that the presence of the inhibitor acts simply by blocking the anodic and cathodic active sites within the covered fraction of the electrode surface without affecting the mechanism of the corrosion reaction. The data duplicated in Table 3 show that the values of  $E_{\text{corr}}$  slightly shift to more positive potentials with increasing the concentration of 1-DMPT. These results suggest that this surfactant functions as a mixed-type inhibitor that acts predominately on the anodic dissolution of the metal [29]. The inhibition efficiency ( $\eta_p$ ) of 1-DMPT obtained its different concentrations and  $25 \text{ }^\circ\text{C}$  was calculated from equation [30]:

$$\eta_p = \frac{j_{\text{corr}} - j_{\text{corr}}^0}{j_{\text{corr}}} \times 100 \quad (5)$$

where  $j_{\text{corr}}$  and  $j_{\text{corr}}^0$  are the corrosion current densities for carbon steel electrode in the uninhibited and inhibited solutions, respectively.

The calculated inhibition efficiencies are listed in Table 3. It is obvious that the inhibition efficiency of 1-DMPT increases with increasing its concentration.

### Ac impedance

EIS provides information on the resistive and capacitive behavior at the interface and makes it possible to evaluate the performance of the test compound as a corrosion inhibitor [30-32]. The impedance data for carbon steel in 1.0 M HCl without and with various concentrations of 1-DMBT were recorded at OCP and 25 °C. Figs. 7 and 8 represent the Nyquist and Bode plots respectively. Nyquist plots consist of capacitive depressed semicircles and often referred to as frequency dispersion. This frequency dispersion can be ascribed to the roughness of the solid surface [33]. The appearance of these of the capacitive semicircles suggests that the corrosion of carbon steel in 1.0 M HCl solution in the absence and presence of 1-DMPT is under charge-transfer control [34].

The addition of the prepared cationic surfactant to acid solution increases the diameter of the semicircle and hence charge transfer resistance ( $R_{ct}$ ) of the corrosion reaction [35,36]. Increasing the concentration of the inhibitor in HCl does not change substantially the shape of the semicircles confirming that this surfactant does not alter the mechanism of the corrosion reaction but inhibits the corrosion processes via increasing the surface coverage of the electrode surface by an isolating adsorption layer of inhibitor. On the other hand, Bode plots involve only one phase maximum revealing that, in all cases, the corrosion reaction is under charge transfer control and the corrosion process occurring through one step corresponds to one time constant [37]. It is clear that, maximum phase angles are less than  $-60^\circ$  indicates the non-ideal capacitive behavior at intermediate frequencies used [38]. Also the maximum phase angle increases and shifts to lower frequencies with increasing the inhibitor concentration, and this may be due to an increase in the surface coverage of the electrode surface by absorbed barrier layer of the inhibitor and consequently a decrease in the surface roughness [39].

The simple Randle's equivalent circuit shown in Fig. 9 was modeled to fit the EIS data [40]. This circuit consists of a parallel combination of a constant phase element (CPE) and the charge transfer resistance ( $R_{ct}$ ) in series connection with the solution resistance ( $R_s$ ). The CPE element is used instead of the pure capacitor to reduce the effect of the roughness and the existence of adsorbed inhibitor species on the electrode surface [41]. CPE element represents the double layer capacitance ( $C_{dl}$ ). The corrosion kinetic parameters as  $R_{ct}$  and  $C_{dl}$  derived from EIS measurements are in given in Table 4.

The inhibition efficiencies ( $\eta_I$ ) were calculated for different concentrations of 1-DMPT at 25 °C using the following equation [42]:

$$\eta_I = \left( \frac{R_{ct} - R_{ct}^0}{R_{ct}} \right) \times 100 \quad (6)$$

where  $R_{ct}^0$  and  $R_{ct}$  are the charge-transfer resistance values in uninhibited and inhibited solutions respectively.

According to the data listed in Table 4. It is seen that value of  $R_{ct}$  increases while that of  $C_{dl}$  decreases with increasing the inhibitor concentration. The inhibition efficiency of 1-DMPT increases with increasing its concentration in the acid solution.

### Weight loss

The corrosion rate ( $k$ ) in  $\text{mg cm}^{-2} \text{h}^{-1}$  and inhibition efficiencies ( $\eta_w$ ) of 1-DMPT were calculated from weight loss measurements for carbon steel in aerated 1.0 M HCl without and with different concentrations of the inhibitor and different temperatures. The inhibition efficiency at any given concentration of the inhibitor and at any given temperature was calculated using the following equation [43]:

$$\eta_w = \frac{W^o - W}{W^o} \times 100 \quad (7)$$

where  $W^o$  and  $W$  are the weight loss of carbon steel in uninhibited and inhibited solution, respectively.

The calculated data are listed in Table 5. Inspection of these data reveals that at a given temperature, the inhibition efficiency ( $\eta_w$ ) enhances with increasing the inhibitor concentration. Moreover, it is seen that the three different techniques gave similar behavior in the absence and presence of the inhibitor. There is an agreement among the inhibition efficiencies  $\eta_p$ ,  $\eta_I$  and  $\eta_w$  of 1-DMPT obtained from the three methods employed.

On the other hand, at one and the same inhibitor concentration, the corrosion rate  $k$ , increases with an increase in temperature indicating the endothermic nature of the carbon steel corrosion in HCl solution. The inhibition efficiency ( $\eta_w$ ) decreases with raising the temperature. This result could be explained on the basis that raising the temperature may shift the adsorption equilibrium towards desorption leading to a decrease in surface coverage and consequently a decrease in inhibition efficiency [44].

### Adsorption thermodynamic

The Langmuir adsorption isotherm was found to fit well with the weight loss data obtained for 1-DMBT. This isotherm is expressed by the following equation at given temperature [45]:

$$\frac{C_{\text{inh}}}{\theta} = \frac{1}{K_{\text{ads}}} + C_{\text{inh}} \quad (8)$$

where  $\theta$  is fractional of the surface coverage ( $\theta = \frac{\eta_w}{100}$ ),  $C_{\text{inh}}$  is the inhibitor concentration, and  $K_{\text{ads}}$  is the equilibrium constant of the adsorption process.

The plot of  $C_{\text{inh}}/\theta$  vs.  $C_{\text{inh}}$  gave a straight line as shown in Fig. 11 with the regression coefficient ( $R^2$ ) higher than 0.9997, this suggests that the experimental data are well described by Langmuir adsorption isotherm. In this case, a single-layer of 1-DMBT species is formed on the electrode surface by the adsorption of the non-planar structure of these

species [46]. Reciprocal of intercepts of the straight line, gave the value of  $K_{\text{ads}}$ . The obtained values of  $K_{\text{ads}}$  are listed in Table 6. It is found that, the value of  $K_{\text{ads}}$  decreases with raising the temperature. These values can be related to the standard Gibbs free energy of adsorption ( $\Delta G^{\circ}_{\text{ads}}$ ) according to the following equation [46]:

$$K_{\text{ads}} = \frac{1}{55.5} \exp\left(\frac{-\Delta G^{\circ}_{\text{ads}}}{RT}\right) \quad (9)$$

where  $R$  is the universal gas constant and  $T$  is the absolute temperature. The value 55.5 is the molar concentration of water.

The high values of  $K_{\text{ads}}$  refer to strong adsorption and good inhibiting effect [47, 48]. The negative values  $\Delta G^{\circ}_{\text{ads}}$  demonstrated that 1-DMPT is spontaneously adsorbed on carbon steel surface [48]. It is suggested that the values of  $\Delta G^{\circ}_{\text{ads}}$  up to  $-20 \text{ kJ mol}^{-1}$  reveal a physisorption while the values around  $-40 \text{ kJ mol}^{-1}$  or smaller reveal a chemisorption [49, 50]. Regarding to the obtained value of  $\Delta G^{\circ}_{\text{ads}}$  ( $35.31$ ,  $35.60$ ,  $36.58$  and  $36.74 \text{ kJ mol}^{-1}$  at  $25, 40, 55$  and  $70 \text{ }^{\circ}\text{C}$ , respectively), it seems that the adsorption of the cationic surfactant 1-DMPT on the carbon steel  $1.0 \text{ M HCl}$  is a mixed physical and chemical adsorption processes [50]. In this case, the chloride and bromide ions are chemically adsorbed on the metal surface. These processes render the electrode surface negatively charge and, therefore, allow electrostatic attraction between the surfactant cation and the electrode surface (physical adsorption). Moreover, the presence of heteroatoms having lone pairs of electrons and  $\pi$ -electrons in 1-DMPT assists the formation of coordinate bonds with vacant d-orbitals of the surface ion atoms (chemisorption) the adsorption enthalpy  $\Delta H^{\circ}_{\text{ads}}$  can be calculated according to the Van't Hoff equation:

$$\ln K_{\text{ads}} = \frac{-\Delta H^{\circ}_{\text{ads}}}{RT} + \text{constant} \quad (10)$$

where  $\Delta H^{\circ}_{\text{ads}}$  and  $K_{\text{ads}}$  are the adsorption enthalpy and adsorption equilibrium constant, respectively.

The plot of  $\ln K_{\text{ads}}$  against  $1/T$  gave a straight line as shown in Fig. 12. From the slope of the line, the value of the standard adsorption enthalpy ( $\Delta H_{\text{ads}}^{\circ}$ ) was calculated and given in Table 6. The negative sign of  $\Delta H_{\text{ads}}^{\circ}$  reflects the exothermic nature of the adsorption process.

Entropy of the inhibitor adsorption ( $\Delta S_{\text{ads}}^{\circ}$ ) was calculated using the following equation:

$$\Delta G_{\text{ads}}^{\circ} = \Delta H_{\text{ads}}^{\circ} - T\Delta S_{\text{ads}}^{\circ} \quad (11)$$

A positive value of  $\Delta S_{\text{ads}}^{\circ}$  is attributed to the increase of disorder and this case may be due to the adsorption of only one surfactant species by desorption of more than one water molecule [50].

#### **Comparison of inhibitory efficiencies of triazole derivatives**

The inhibitory efficiency of the synthesized cationic surfactant (1-DMBT) with those of previously published triazole derivatives are comparatively for carbon steel corrosion in 1 M HCl solution [48,49,51,52] are listed in Table 7. As can be seen in this table the inhibitory efficiencies of the synthesized cationic surfactant are comparable to or better than those of previously reported triazole derivatives at the same condition. The synthesized 1-DMPT is better than those of literature reported triazole derivatives at the same condition because 1-DMPT is a cationic surfactant based on triazole derivative, however, most triazole derivatives reported in the literature are ordinary organic compounds. Surfactants that lower the surface tension (or interfacial tension) between corrosive medium and steel surface and also act as dispersants. Surfactants are amphiphilic as they contain both hydrophobic groups (their tails) and hydrophilic groups (their heads) [53]. Therefore, surfactants up to critical micelle concentration ( $C_{\text{cmc}}$ ) will diffuse out of the bulk water phase and are adsorbed at the interfaces between carbon steel and corrosive medium. On the other side, organic compounds will diffuse both in bulk solution and interface by the same rate nearly. In addition, surfactant



up to  $C_{cmc}$  form thin film on steel surface involved two inhibitive factors; one hydrophilic group involved hetero atoms and other water-insoluble hydrophobic group.

#### 4. Conclusions

The novel cationic surfactant 1-DMPT was synthesized in our laboratory and its structure was confirmed by using  $^1\text{H}$  NMR,  $^{13}\text{C}$  NMR and FTIR spectroscopic analysis and some of its surface properties reveal that 1-DMPT acts a good surface active agent.

The inhibition function of this surfactant for the corrosion of carbon steel in 1.0 M HCl was studied by three different techniques, namely potentiodynamic polarization, EIS, and weight loss. The results obtained from the three techniques are similar and in a reasonable good agreement. The results reveal that 1-DMPT acts as a good corrosion inhibitor for carbon steel in HCl medium. The inhibitor acts as a mixed-type inhibitor and its inhibition is due to the adsorption and formation of an insulator layer on the electrode surface. The inhibitor efficiency of this inhibitor increases with increasing its concentration but decrease with increasing temperature. The thermodynamic parameters of adsorption,  $\Delta G^\circ_{ads}$ ,  $\Delta H^\circ_{ads}$  and  $\Delta S^\circ_{ads}$  reveal that the adsorption of 1-DMPT on carbon steel surface is physically and chemically together and obeys Langmuir isotherm.

#### References

1. Issaadi S, Douadi T, Zouaoui A, Chafaa S, Khan MA, Bouet G (2011) Corros. Sci. 53: 1484-1488.
2. Tang Y, Yang X, Yang W, Chen Y, Wan R (2010) Corros. Sci. 52: 242-249.
3. Li X, Deng S, Fu H (2011) Corros. Sci. 53: 3241-3247.
4. Li X, Deng S, Fu H (2011) Corros. Sci. 53: 302-309.

5. Döner A, Solmaz R, zcan M, Kardas G (2011) *Corros. Sci.* 53: 2902-2913.
6. Hegazy MA, Badawi AM, Abd El Rehim SS, Kamel WM (2013) *Corros. Sci.* 69: 110-122.
7. Tourabi M, Nohair K, Traisnel M, Jama, Bentiss F (2013) *Corros. Sci.* 75: 123-133.
8. Sastri VS, *Corrosion Inhibitors – Principles and Applications*, Wiley, Chichester, England, 1998
9. Hegazy MA, El-Tabei AS, Ahmed HM (2012) *Corros. Sci.* 64: 115-125.
10. El-Tabei AS, Hegazy MA, Bedair AH, Sadeq MA (2014) *J Surfact. Deter.* 17: 341-352.
11. Lalitha A, Ramesh S, Rajeswari S (2005) *Electrochim. Acta* 51: 47-55.
12. Hegazy MA, Abdallah M, Awad MK, Rezk M (2014) *Corros. Sci.* 81: 54-64.
13. Amin MA, Abd El-Rehim SS, El-Sherbini EEF, Bayyomi RS (2007) *Electrochim. Acta* 52: 3588-3600.
14. Mohamed HM, Mohamed El-Hady F, Hassan Shehata AH, Hegazy MA, Hassan Hefni HH (2013) *J Surfact. Deter.* 16: 233-242.
15. Shams El Din AM, Mohammed RA, Haggag HH (1997) *Desalination* 114: 85-95.
16. El-Ashry EH, El-Nemr A, Esawy SA, Ragab S (2006) *Electrochim. Acta* 51: 3957-3968.
17. Wang H-L, Liu R-B, Xin J (2004) *Corros. Sci.* 46: 2455-2466.
18. Tamilselvi S, Rajeswari S (2003) *Anti-Corros. Meth. Mater.* 50: 223-231.
19. Wang H-L, Fan H-B, Zheng J-S (2003) *Mater. Chem. Phys.* 77: 655-661.
20. Musa AY, Kadhum AAH, Mohamad AB, Takriff MS, Daud AR, Kamarudin SK (2010) *Corros. Sci.* 52: 526-533.
21. Zheludkevich ML, Yasakau KA, Poznyak SK, Ferreira MGS (2005) *Corros. Sci.* 47: 3368-3383.
22. Tourir R, Dkhireche N, Ebn Touhami M, Lakhrissi M, Lakhrissi B, Sfaira M, Part I: EIS study (2009) *Desalination* 249: 922-928.

23. Kelly RG, Scully JR, Shoesmith DW, Buchheit RG (2003) *Electrochemical Techniques in Corrosion Science and Engineering*, Marcel Dekker, Inc., New York, 127, 290:302
24. Bockris J, Reddy AKN, Gamboa-Aldeco M (2000) *Modern Electrochemistry*. pp. 871-890, 973-975.
25. Ostovari A, Hoseinieh SM, Peikari M, Shadizadeh SR, Hashemi SJ(2009) *Corros. Sci.* 51: 1935-1949.
26. Morad MS, Sarhan AAO (2008) *Corros. Sci.* 50: 744-753.
27. John S, Joseph B, Aravindakshan KK, Joseph A (2010) *Mater. Chem. Phys.* 122: 374-379.
28. Jacob KS, Parameswaran G (2010) *Corros. Sci.* 52: 224-228.
29. Ahamad I, Quraishi M (2009) *Corros. Sci.* 51: 2006-2013.
30. Zhang S, Tao Z, W Li, Hou B (2009) *Appl. Surf. Sci.* 255: 6757-6763.
31. Outirite M, Lagrenee M, Lebrini M, Traisnel M, Jama C, Vezin H, Bentiss F (2010) *Electrochim. Acta* 55: 1670-1681.
32. Badr GE (2009) *Corros. Sci.* 51: 2529-2536.
33. Palomar-Pardavé M, Romero-Romo M, Herrera-Hernández H, Abreu-Quijano MA, Natalya- Likhanova V, Uruchurtu J, Jurez-García JM (2012) *Corros. Sci.* 54: 231-243.
34. Khaled KF, Hackerman N (2003) *Mater. Chem. Phys.* 82: 949-960.
35. Bentiss F, Outirite M, Traisnel M, Vezin H, Lagrenee M, Hammouti B, Al-Deyab SS, Jama C (2012) *Int. J. Electrochem. Sci.* 7: 1699-1723.
36. Ahamad I, Prasad R, Quraishi MA (2010) *Corros. Sci.* 52: 1472-1481.
37. Abdel-Rehim SS, Ibrahim MAM, Khaled KF (2001) *Mater. Chem. Phys.* 70: 268-273.
38. El-Tabei AS, Hegazy MA (2013) *J Surfact. Deterg.* 16: 757-766.
39. El-Tabei AS, Hegazy MA, (2013) *J Surfact. Deterg.* 16: 221-232.

40. Oguzie EE, Njoku VO, Enenebeaku CK, Akalezi CO, Obi C (2008) *Corros. Sci.* 50: 3480-3486.
41. Bouklah M, Hammouti B, Lagrenee M, Bentiss F (2006) *Corros. Sci.* 48: 2831-2842.
42. Elayyachy M, El Idrissi A, Hammouti B (2006) *Corros. Sci.* 48: 2470-2479.
43. Bentiss F, Lebrini M, Vezin H, Chai F, Traisnel M, Lagrenee M (2009) *Corros. Sci.* 51: 2165-2173.
44. Goulart CM, Esteves-Souza A, Martinez-Huitle CA, Rodrigues CJF, Maciel MAM, Echevarria A (2013) *Corros. Sci.* 67: 281-291.
45. Solmaza R, Kardas G, Culha M, Yazıcı B, Erbil M (2008) *Electrochim. Acta* 53: 5941-5952.
46. Singh AK, Quraishi MA (2011) *Corros. Sci.* 53: 1288-1297.
47. Bahrami MJ, Hosseini SMA, Pilvar P (2010) *Corros. Sci.* 52: 2793-2803.
48. Quraishi MA, Sudheer KR, Eno Ebenso E (2012) *Int. J. Electrochem. Sci.* 7: 7476-7492.
49. Kumar MS, Ashok Kumar SL, Sreekanth A (2012) *Ind. Eng. Chem. Res.* 51: 5408-5418.
50. Schweinsberg D, George G, Nanayakkara A, Steinert D (1988) *Corros. Sci.* 28: 33-42.
51. El Mehdi B, Mernari B, Traisnel M, Bentiss F, Lagrenee M (2003) *Mater. Chem. Phys.* 77: 489-496.
52. Bentiss F, Bouanis M, Mernari B, Traisnel M, Vezin H, Lagrenee M (2007) *Appl. Surf. Sci.* 253: 3696-3704.
53. Rosen MJ and Kunjappu JT (2012) *Surfactants and Interfacial Phenomena* (4th ed.) Hoboken, New Jersey: John Wiley & Sons. p. 1.

### **Caption of figures**

Fig. 1. The chemical structure of the prepared cationic surfactant.

Fig. 2. <sup>1</sup>HNMR spectrum of 1-DMBT.

Fig. 3.  $^{13}\text{C}$ NMR spectrum of 1-DMBT.

Fig. 4. FTIR spectrum of 1-DMBT.

Fig. 5. Variation of the surface tension with logarithm concentration of the prepared cationic surfactant in water at 25 °C.

Fig. 6. The specific conductivity against concentrations of the prepared cationic surfactant in water at 25 °C.

Fig. 7. Nyquist plots for carbon steel in 1.0 M HCl in the absence and presence of different concentrations of 1-DMBT at 25 °C.

Fig. 8. The suggested equivalent circuit model for the studied system.

Fig. 9. Bode and Phase diagrams for carbon steel in 1.0 M HCl in the absence and presence of different concentrations of 1-DMBT at 25 °C.

Fig. 10. Anodic and cathodic polarization curve for carbon steel in 1.0 M HCl in the absence and presence of different concentrations of 1-DMBT at 25 °C.

Fig. 11. Influence Temperature difference for carbon steel in 1.0 M HCl in the absence and presence of different concentrations of 1-DMBT

Fig. 12. Langmuir's adsorption plots for carbon steel in 1.0 M HCl containing different concentrations of 1-DMPT at 25 °C.

Fig. 13. The relation between  $\ln K_{\text{ads}}$  and  $1/T$  for carbon steel in 1.0 M HCl containing different concentrations of 1-DMPT at 25 °C.

**Table 1**

Chemical composition of carbon steel sample

Element	C	Si	P	S	Ni	Mo	V	Al	Fe
Content (wt. /wt.)%	0.07	0.18	0.03	0.06	0.02	0.004	0.002	0.04	Rest

**Table 2**

Surface parameters of the synthesized cationic surfactant using surface tension and specific conductivity measurements at 25 °C

Property	Surface tension measurements					Conductivity measurements		
	$C_{cmc}$	$\gamma_{cmc}$	$\pi_{cmc}$	$\Gamma_{max} \times 10^{10}$	$A_{min}$	$C_{cmc}$	$\beta$	$\Delta G^{\circ}_m$
	M	mN m <sup>-1</sup>	mN m <sup>-1</sup>	mol cm <sup>-2</sup>	nm <sup>-2</sup>	M		kJ mol <sup>-1</sup>
Value	0.0042	29	43	2.5	0.64	0.0045	0.322	-20.58

**Table 3**

Potentiodynamic polarization parameters for carbon steel corrosion in 1.0 M HCl in the absence and presence of different concentrations of the synthesized 1-DMBT at 25 °C

Conc. of inhibitor	$E_{\text{corr}}$	$j_{\text{corr}}$	$\beta_a$	$\beta_c$	$\eta_p$
M	mV(Ag/AgCl)	mA cm <sup>-2</sup>	mV dec <sup>-1</sup>	mV dec <sup>-1</sup>	%
0.00	-457	1.736	176	152	-
5x10 <sup>-5</sup>	-449	0.997	185	154	42.6
1x10 <sup>-4</sup>	-447	0.849	189	151	51.1
5x10 <sup>-4</sup>	-443	0.337	169	145	80.6
1x10 <sup>-3</sup>	-442	0.195	193	149	88.8
5x10 <sup>-3</sup>	-440	0.145	197	148	91.2



**Table 4**

EIS parameters for corrosion of carbon steel in 1.0 M HCl in the absence and presence of different concentrations of the synthesized 1-DMBT at 25 °C

Conc. of inhibitor	$R_s$	$Y_o$	$n$	Error of $n$	$R_{ct}$	$\eta_i$
M	$\Omega \text{ cm}^2$	$\mu\Omega^{-1}\text{s}^n \text{ cm}^{-2}$		%	$\Omega \text{ cm}^2$	%
0.00	1.8	426	0.73	0.4	71	-
$5 \times 10^{-5}$	1.4	271	0.73	0.5	159	55.3
$1 \times 10^{-4}$	2.0	226	0.70	0.5	195	63.6
$5 \times 10^{-4}$	1.8	156	0.70	0.5	499	85.8
$1 \times 10^{-3}$	1.5	136	0.70	0.4	716	90.1
$5 \times 10^{-3}$	1.5	102	0.71	0.6	1195	94.1

**Table 5**

Weight loss data for carbon steel 1.0 M HCl in the absence and presence of different concentrations of the synthesized (1-DMBT) at various temperatures

Inhibitor Conc. (M)	25 °C			40 °C			55 °C			70 °C		
	$k$ mg cm <sup>-2</sup> h <sup>-1</sup>	$\theta$	$\eta_w$ %	$k$ mg cm <sup>-2</sup> h <sup>-1</sup>	$\theta$	$\eta_w$ %	$k$ mg cm <sup>-2</sup> h <sup>-1</sup>	$\theta$	$\eta_w$ %	$k$ mg cm <sup>-2</sup> h <sup>-1</sup>	$\theta$	$\eta_w$ %
-	1.2000	-	-	2.4000	-	-	3.5740	-	-	7.7000	-	-
1×10 <sup>-5</sup>	0.5761	0.519	51.9	1.6006	0.333	33.3	2.6348	0.262	26.2	6.3487	0.192	19.2
5×10 <sup>-5</sup>	0.2530	0.789	78.9	0.7602	0.683	68.3	1.6001	0.552	55.2	4.3924	0.429	42.9
1×10 <sup>-4</sup>	0.0609	0.910	91.0	0.2118	0.873	87.3	0.6543	0.767	76.7	2.6891	0.710	71.0
5×10 <sup>-4</sup>	0.0431	0.948	96.4	0.2319	0.903	90.3	0.4928	0.836	83.6	1.7357	0.774	77.4
1×10 <sup>-3</sup>	0.0315	0.973	97.3	0.1581	0.945	94.5	0.3834	0.892	89.2	1.3575	0.836	83.6

**Table 6**

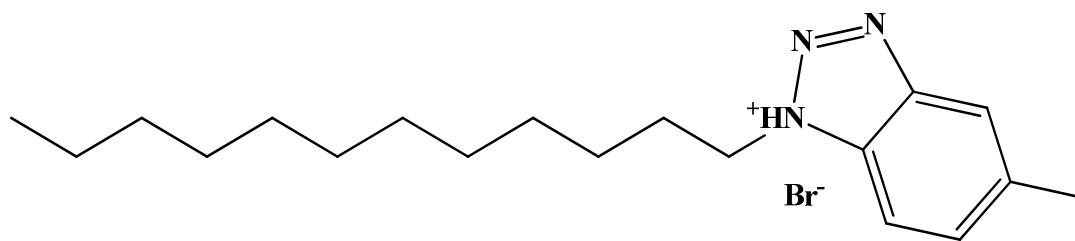
Standard thermodynamic parameters of the adsorption on carbon steel surface in 1 M HCl containing different concentrations of the synthesized 1-DMBT at various temperatures

Temperature °C	$K_{\text{ads}}$ M <sup>-1</sup>	$\Delta G^{\circ}_{\text{ads}}$ kJ mol <sup>-1</sup>	$\Delta H^{\circ}_{\text{ads}}$ kJ mol <sup>-1</sup>	$\Delta S^{\circ}_{\text{ads}}$ Jmol <sup>-1</sup> K <sup>-1</sup>
25	27855.15	-35.31	-34.65	118.36
40	15723.27	-35.60		113.61
55	9871.67	-36.58		111.42
70	7022.47	-36.74		106.92

**Table 7**

Comparison between inhibition efficiency of the synthesized cationic surfactant based on tolyltriazole derivatives investigated as corrosion inhibitors by other authors at the same conditions

Inhibitor name	Inhibition efficiency (%)	Reference
4-amino-5-(2-hydroxy)phenyl-4H-1,2,4,-triazole-3-thiol (AHPTT)	70.5	[48]
4-amino-5-styryl-4H-1,2,4,-triazole-3-thiol (ASTT)	76.7	[48]
4-salicylideneamino-3-methyl-1,2,4-triazole-5-thione(SAMTT)	76.0	[49]
4-(2,4-dihydroxybenzylideneamino)-3-methyl-1H-1,2,4-triazole-5(4H)-thione (DBAMTT)]	79.0	[49]
3,5-di(m-tolyl)-4H-amino-1,2,4-triazole (m-DTAT)	63.8	[51]
3,5-di(m-tolyl)-4-amino-1,2,4-triazole (m-DTAT)	86.9	[51]
3,5-diphenyl-4H-1,2,4-triazole (DHT)	84.1	[52]
1-dodecyl-methyl-1 <i>H</i> -benzo[ <i>d</i> ][1,2,3]triazole-1-ium bromide	94.1	This work



**1-dodecyl-5-methyl-1*H*-benzo[*d*][1,2,3]triazol-1-ium bromide**

**Fig. 1**

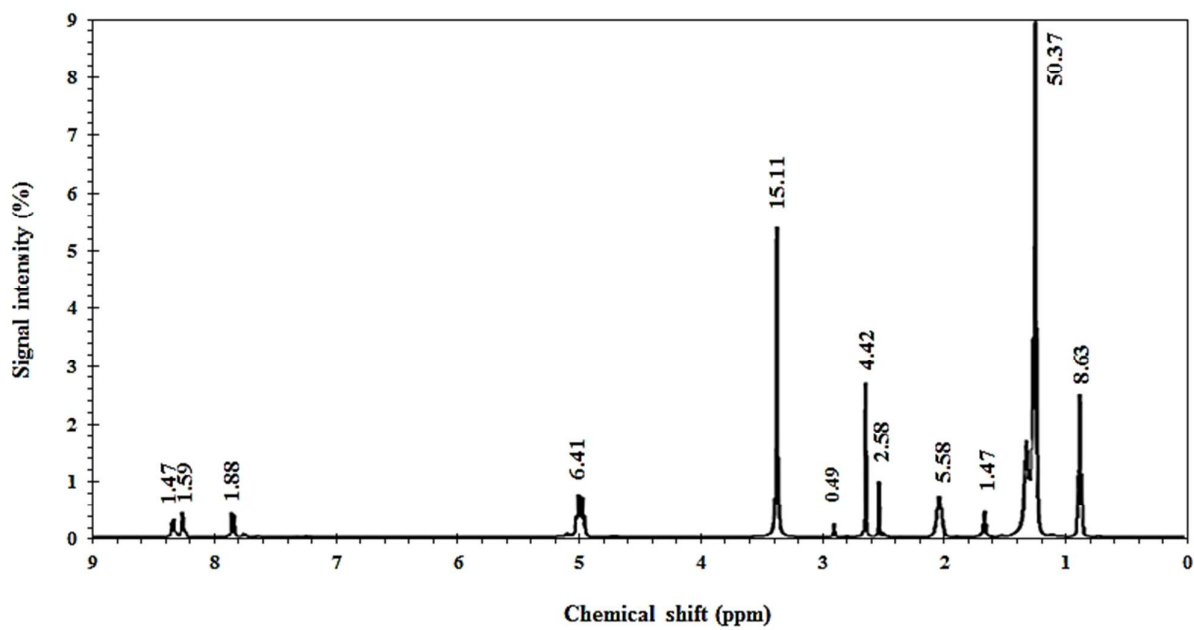


Fig. 2

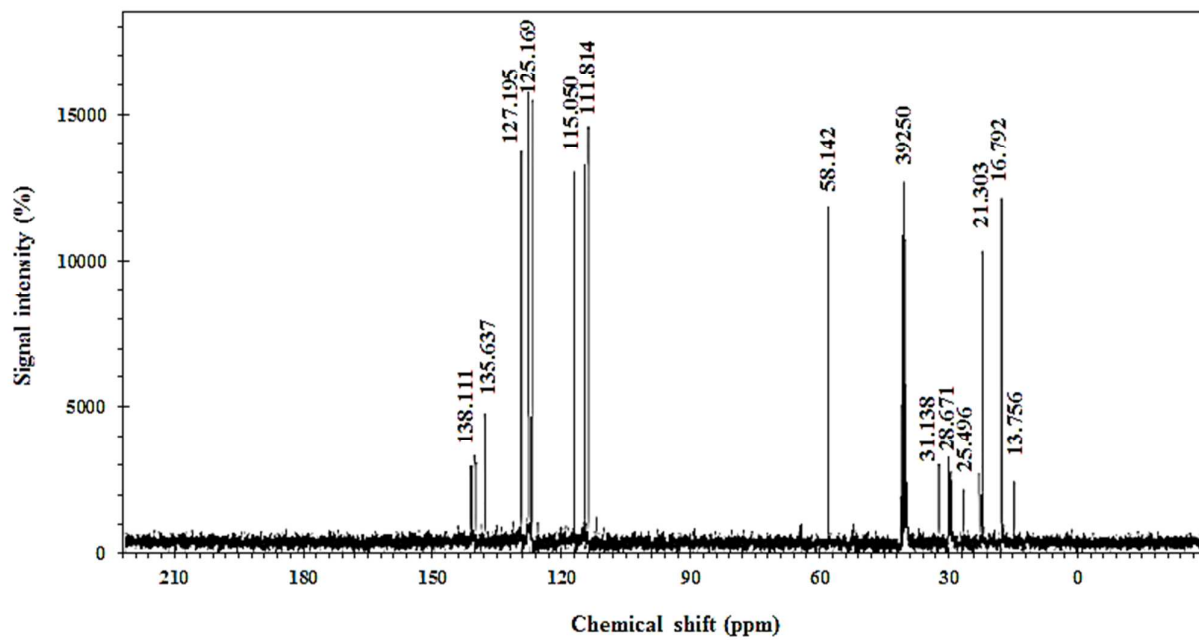


Fig. 3

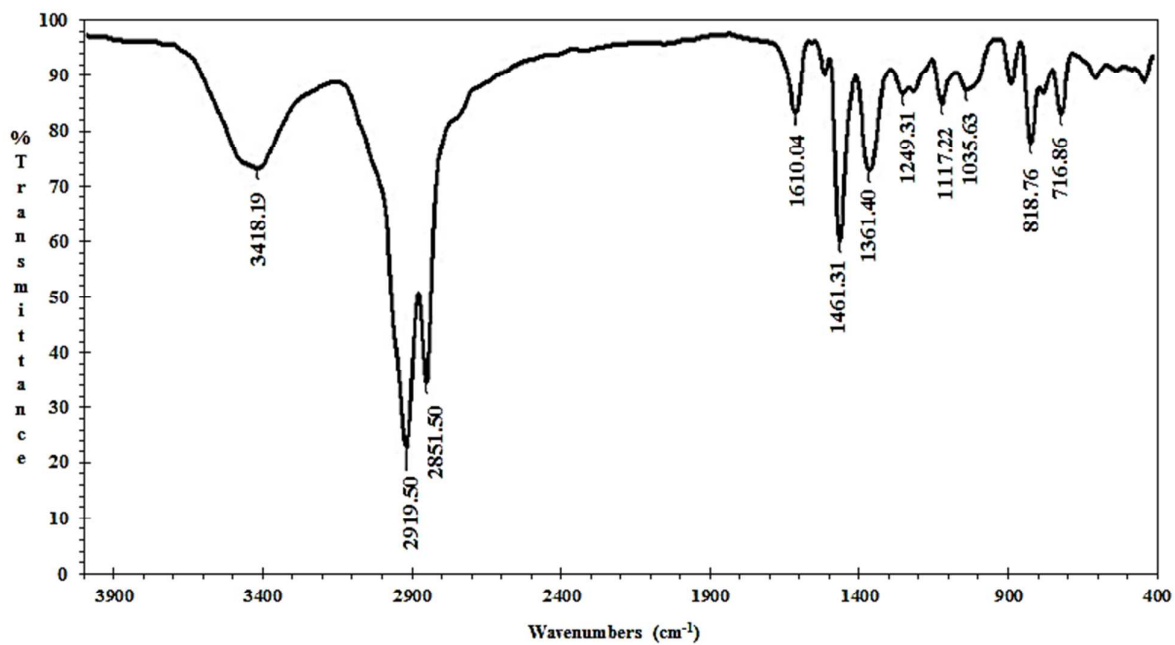


Fig. 4



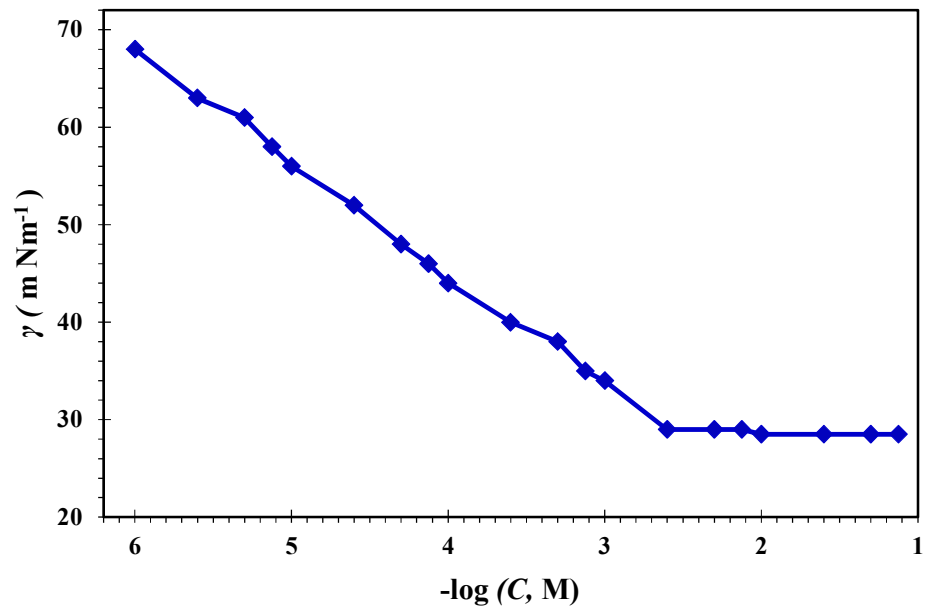


Fig. 5

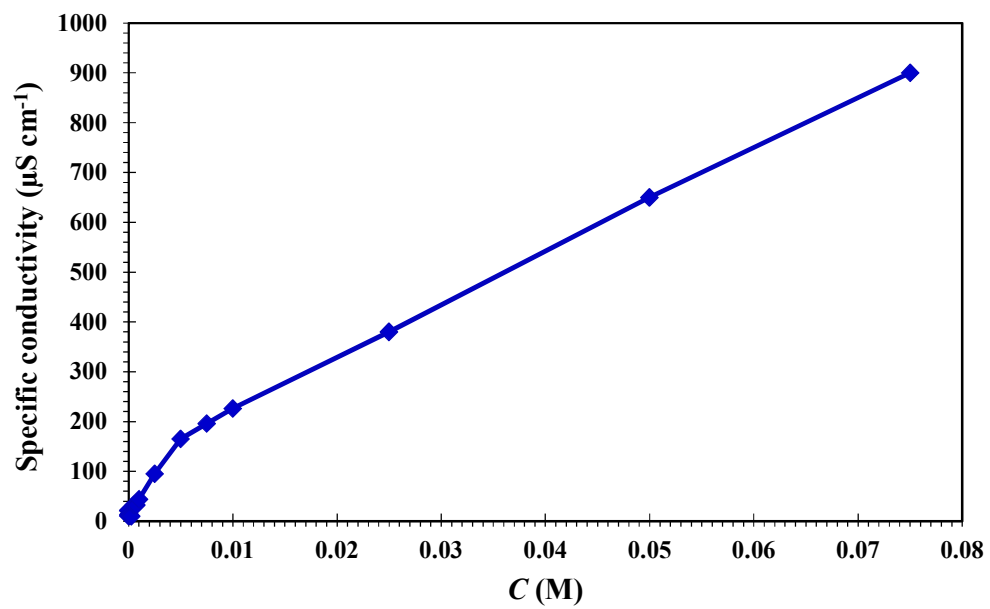


Fig. 6

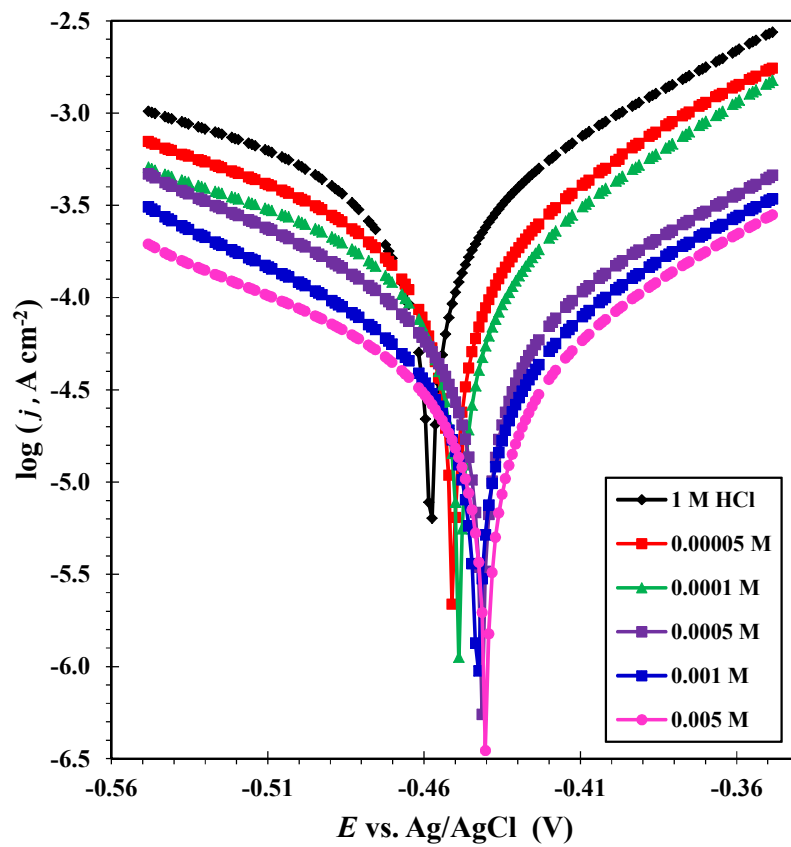


Fig. 7

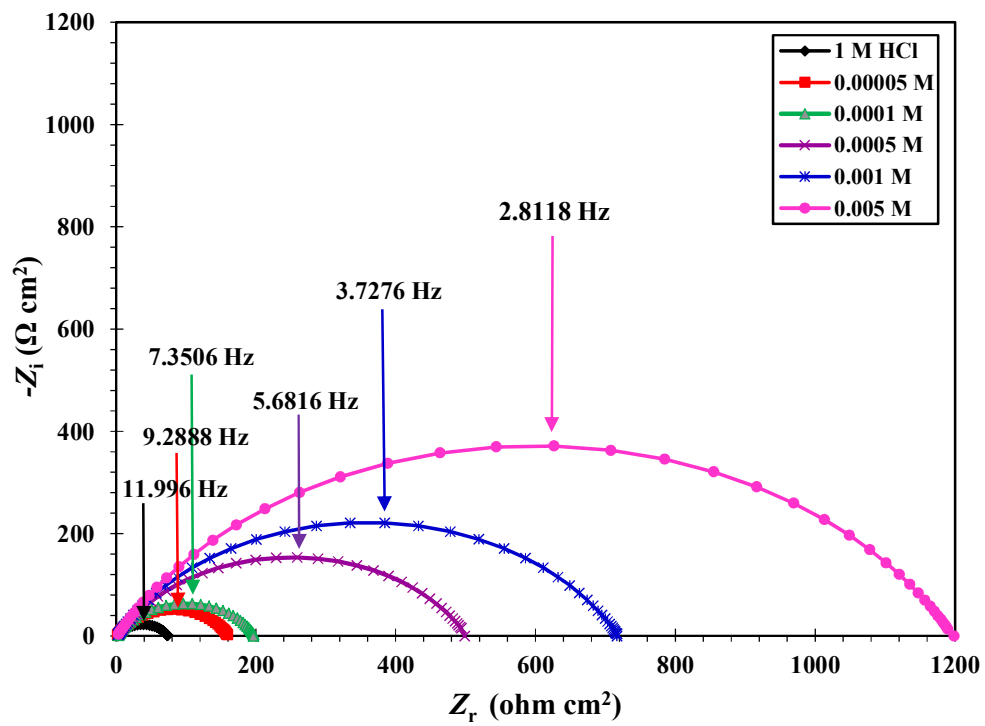


Fig. 8

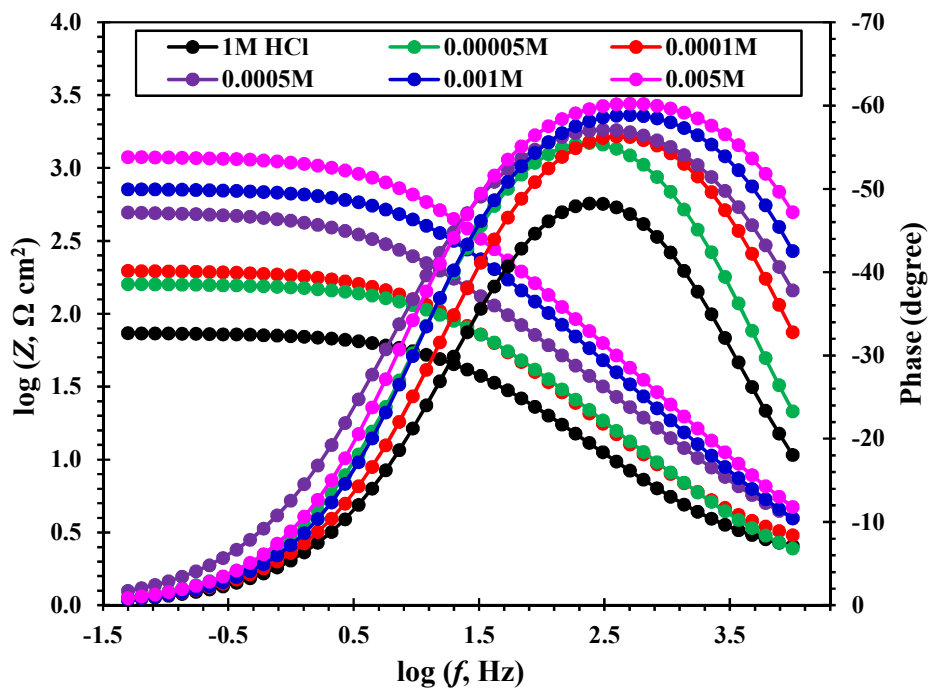


Fig. 9

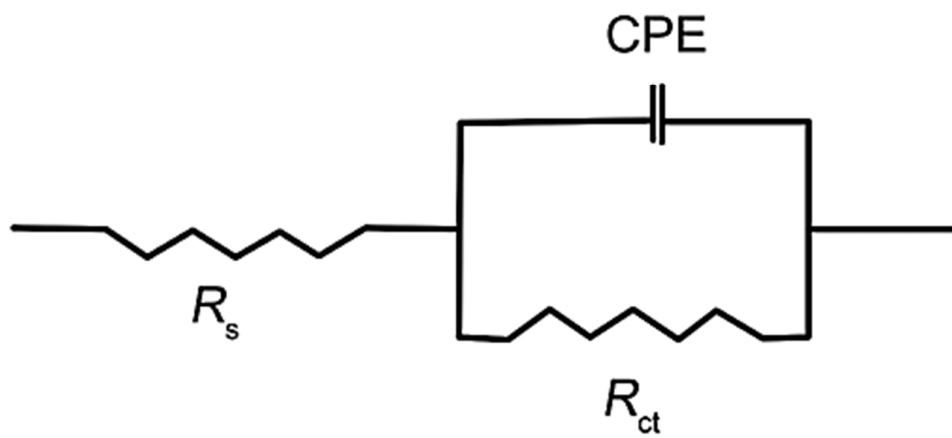


Fig. 10

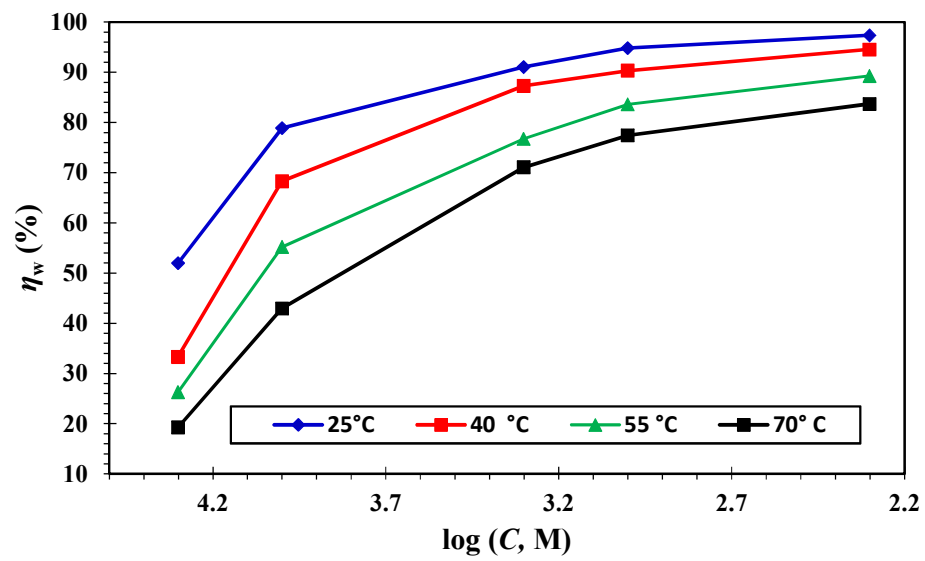


Fig. 11

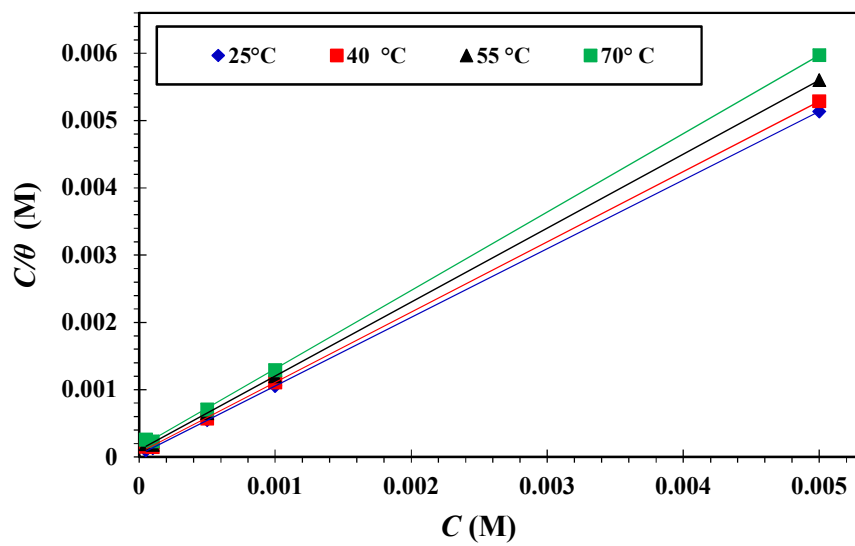


Fig. 12



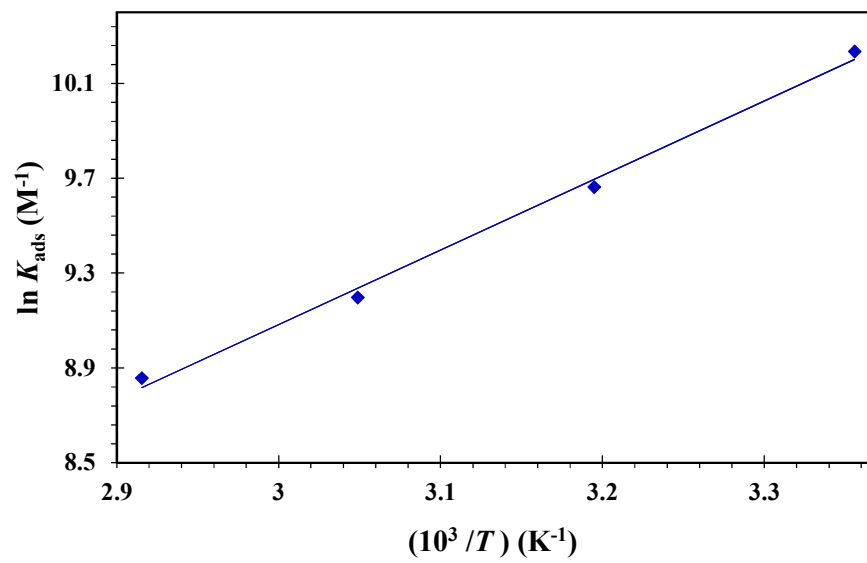


Fig. 13